

SINGLE MASK LATERAL TUNNELING ACCELEROMETER

P. G. Hartwell¹, F. M. Bertsch¹, S. A. Miller², K. L. Turner³, and N. C. MacDonald¹

¹School of Electrical Engineering, ²School of Applied and Engineering Physics,

³Department of Theoretical and Applied Mechanics

Cornell University, Ithaca, NY, 14853-5401 USA

pgh1@cornell.edu

ABSTRACT

A single-mask lateral tunneling accelerometer with integrated tip has been developed and characterized. High aspect ratio single-crystal silicon springs provide high resolution, wide operating bandwidth, and excellent isolation from off-axis stimuli. In this paper, we present the first such device implementing the SCREAM [1] process technology. We focus on the advantages that this technology affords tunneling accelerometers and present a typical high-resolution accelerometer with 20 μg / rt Hz performance at 100 Hz and 5.5 kHz resonant frequency.

INTRODUCTION

The ability to measure and quantify the motion of an object is one of the most basic senses required in advanced control systems. Accelerometers have been used in many recent applications from automobiles to airplanes to computer interfaces. Previously, high resolution accelerometers have been large and expensive to manufacture creating a market for a new design and manufacturing methodology, such as micromachining. Many micromachined accelerometers have been developed. [2] A subset of these use the electron tunneling phenomenon as the high-gain transducer, an idea first implemented in 1988 [3]. Although designs vary greatly, all employ a tunneling tip which is proximal to a proof mass.

The most common designs for tunneling accelerometers use several bulk micromachined wafers bonded together [4,5,6,7]. These accelerometers are sensitive in the Z-axis, normal to the wafer, and their parameters are very susceptible to process variations and require high voltages for actuation.

Other designs for cantilevered devices [8] and lateral devices [9] have also been presented. Previous lateral devices have been fabricated with surface micromachining. The limitations on depth of polysilicon structures result in devices with low proof masses and poor off-axis isolation.

Devices fabricated using the SCREAM bulk micromachining process do not have many of the problems associated with earlier designs. The nature of the SCREAM process allows the device characteristics to be precisely matched to the specific application. Important parameters such as proof mass, spring constants, and actuation force can be independently varied. These device properties are directly defined in the single lithography step and are independent of most minor processing variations. Devices can be specifically designed for bandwidth, resolution, or a combination of both. This freedom allows devices to be

fabricated for seismic and acoustic applications (nano-g or micro-g resolution) as well as automotive and aerospace applications (milli-g resolution, tens of kHz bandwidth). High aspect ratio structures typical of SCREAM allow for accelerometer designs which have low off-axis sensitivity and large proof masses. Devices have been designed with proof masses from 5 micrograms to 2 milligrams and spring constants from 0.5 - 50 N/m, allowing a maximum resolution of 70 ng/rt Hz. One sample accelerometer is presented and characterized here.

BASIC THEORY

In tunneling accelerometers, a metal-coated tip is brought to within a nanometer of a spring-supported proof mass. If a small bias voltage, typically 100 mV, is applied to the tip, a current will tunnel across the separation. Applied acceleration causes a relative displacement of the spring-supported proof mass, and a change in the tunneling current, according to the exponential dependence shown in Equation 1. To improve the dynamic range of this sensor, force feedback is used to maintain a constant tunneling current, typically about 1 nA. In this case, an electrostatic force is used to control the position of the proof mass. Since the relative position of the mass must be a constant to keep the tunnel current constant, the sum of the electrostatic and inertial force on the mass must be a constant. Therefore, variations in the inertial force due to acceleration can be detected by monitoring changes in the electrostatic balancing force

$$I_t \propto V_b \exp(-\alpha x \sqrt{\phi}) \quad [1]$$

where x =separation, ϕ =barrier height, α =tunneling constant ($\alpha=1.025 \text{ 1}/(\text{\AA} \sqrt{\text{eV}})$), and V_b =bias voltage.

DESIGN GEOMETRY AND SPECIFICATIONS

The basic design for a lateral tunneling accelerometer fabricated with the SCREAM process contains a proof mass which is suspended by four springs as seen in Figure 1. The tunneling junction is created by moving the proof mass towards a fixed lateral tunneling tip using an integrated electrostatic actuator. The 'tip' used in this accelerometer is actually a wedge shaped beam formed by the standard process. The exponential nature of electron tunneling insures that tunneling current will be dominated by the two atoms in closest proximity on the tunneling electrodes, i.e. the tip and the proof mass. Imaging with a scanning tunneling microscope, STM, requires precise knowledge of XYZ position which is accomplished by tunneling with a precisely positioned atomically sharp tip. However, to use tunneling in acceleration sensing, only knowledge of ΔX is required.

This allows us to use a wedge-shaped beam instead of needing an atomically sharp tip as is typically used for tunneling. A SEM image of the ‘tip’ is shown in Figure 2.

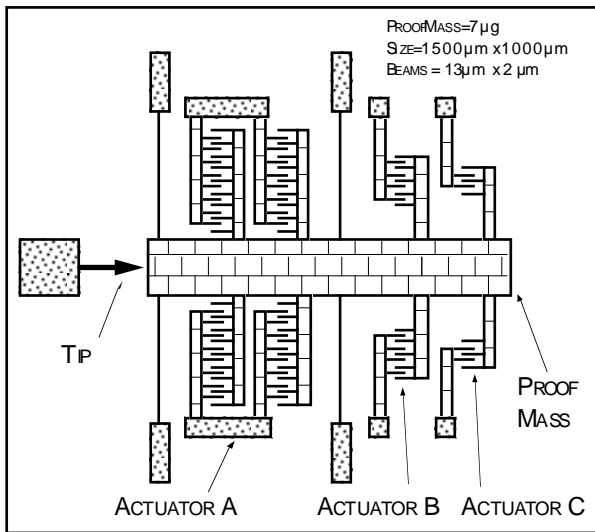


Fig. 1 Schematic of a lateral tunneling accelerometer.

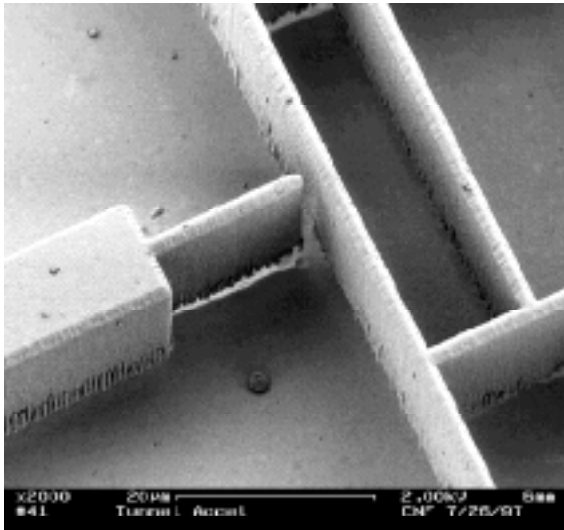


Fig. 2 SEM of integrated tunneling tip, showing tip/proof mass interface. Device is at rest position.

The actuators on the proof mass are designed to provide sufficient force to allow device operation using reasonable integrated circuit voltages. The tip-proof mass rest gap is about 1.2 μm . Actuator A, with 500 electrostatic comb fingers can close this gap with a 15V bias voltage. Self-test actuators are included for in-situ device performance verification. These are seen as actuators B and C in Figure 1. Actuator B with 50 comb fingers can provide sufficient movement with 15V to simulate up to a 9 g excitation. Actuator C has 5 comb fingers and can be used for smaller self test excitations or fine control of proof mass movement.

The design shown in Figure 3 has a proof mass of 7.0 micrograms. The suspension springs are each 200 μm long, 2 μm wide and 13 μm deep. This gives a theoretical spring constant in the sensitive direction of 6 N/m. Proof mass and spring constant have been

measured at 5.2 micrograms and 6.2 N/m, respectively. In the out of plane Z direction, the calculated spring constant is 140 N/m. This should provide excellent isolation from off-axis excitations. From these numbers a theoretical fundamental natural frequency can be calculated to be 4.6 kHz, close to the measured value of 5.5 kHz.

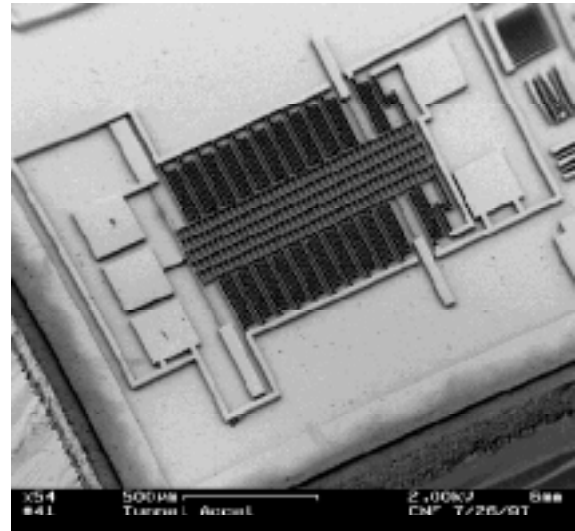


Fig. 3 SEM of lateral tunneling accelerometer.

FABRICATION

Lateral tunneling accelerometers have been fabricated using the SCREAM [1] bulk micromachining process. A silicon dioxide mask is patterned with a photolithography step. This mask is then used to etch 10-20 μm into the single crystal silicon substrate. A passivating PECVD silicon dioxide film is deposited over the entire wafer and then anisotropically etched to remove it from the floors of trenches. Then an isotropic RIE silicon etch is used to under-cut small width features (beams) releasing them from the substrate. Features wider than a characteristic size remain anchored to the substrate. The released structures are then conformally coated with an aluminum film.

Aluminum oxidizes readily and is not a suitable material for tunneling. Typically, noble metals, such as gold, which do not form native oxides, are used. The aluminum/gold system is notorious for degrading with the formation of Al/Au intermetallics, commonly known as the “purple plague.” [10] To avoid this, the aluminum coated devices are allowed to oxidize over night forming a native alumina coating over the structures. A gold layer is then evaporated over the entire wafer, using a rotating stage at an oblique angle to the source. This provides good coverage of the electrostatic comb fingers and the tunnel junction.

Alumina is well known as a stable material and a good diffusion barrier. Adhesion of gold to the alumina has been found to be adequate. Devices with this metal system have been tested as operational for six months of periodic testing. Auger analysis of the gold surface after six months shows no signs of aluminum or silicon having migrated to the gold surface

DEVICE CHARACTERIZATION

This accelerometer was characterized following guidelines described by Liu, *et. al.* [11]. Experiments confirmed device tunneling and mechanical and electrical performance consistent with expectations.

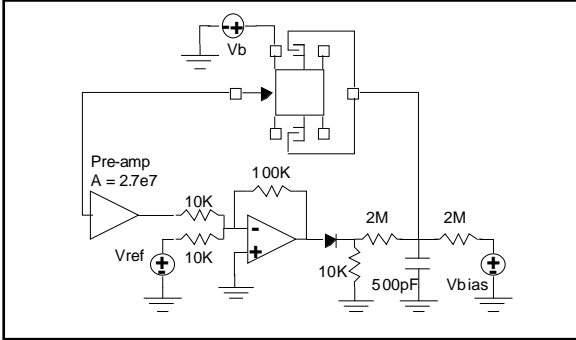


Fig. 4 Feedback circuit for controlling lateral tunneling accelerometer.

The tunneling accelerometer is controlled with the simple feedback circuit shown in Figure 4. The tunneling current is fed into a transresistance amplifier with high gain. This voltage signal is then compared to a reference signal proportional to the desired tunneling current. An error signal is determined and then summed with a large signal actuator bias to control the tunnel gap. The gap is therefore controlled to a separation defined by the reference setpoint. Fluctuations in the gap, caused by physical excitation of the proof mass cause an error signal to be generated which can be monitored to describe the physical excitation experienced by the system.

To demonstrate that the system is in fact tunneling, two experiments were performed. In the first, the system is taken out of a feedback mode. The tunnel gap is adjusted with actuator A and the tunnel current is monitored. A plot of tunnel current versus separation shows the characteristic log dependence of Equation 1. This data is presented in Figure 5.

A second experiment, first presented by Kenny [12], involves modulating the tunnel current reference signal with a 100 Hz sine wave. This modulation will effectively cause a modulation of the tunnel current which is a mixture of the sine wave and the exponential dependence on tunnel gap. The two waveforms are seen in Figure 6, with sine and sine/exponential shapes. When plotted against each other, the results are again seen to follow the exponential behavior of Equation 1. This result can be seen in Figure 7.

From these two verifications of tunneling, the effective tunnel barrier height for the system can be extracted. By solving equation 1 for our log plot:

$$\ln\left(\frac{I_t}{V_b}\right) = (-\alpha\sqrt{\phi})x \quad [2]$$

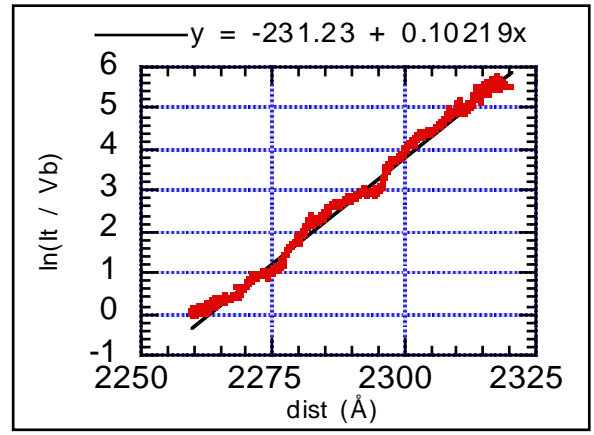


Fig. 5 Plot of tunneling current (I) vs. tip/proof mass separation.

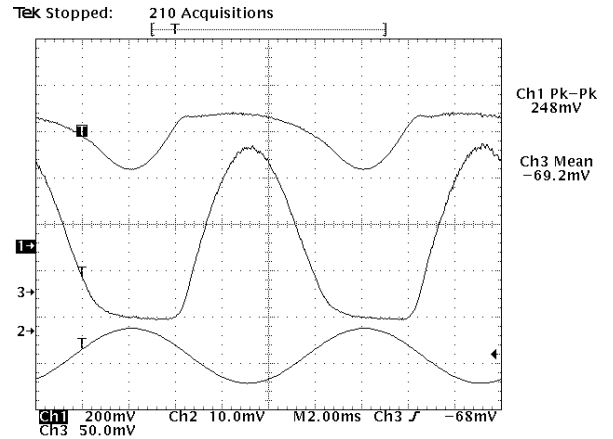


Fig. 6 Sinusoidal modulation of tunneling current reference. Bottom trace shows excitation, middle trace shows exponential dependence of current superimposed on sine wave excitation. Top trace shows error signal of feedback control circuit in response to modulation.

The slope of the linear plots in Figures 5 and 7 gives a measured tunnel barrier height of 0.006 eV. This is less than the typically quoted value of 0.2 eV to 0.5 eV for gold surfaces in tunneling accelerometers. One possible source of discrepancy is our inability to accurately measure the distance/voltage relationship of actuator A. To determine ordinate values in Figure 5 and 7, we have used a theoretical value based on calculations of capacitance of the fingers of the comb motor and theoretical spring constants. Experiments have shown that while tunneling, the proof mass natural frequency is increased to 8.6 kHz. This is a result of force feedback on the system and appears as a stiffening of the system that reduces the effectiveness of actuator A. This causes artificially low work functions to be calculated. An experiment is being designed to use laser interferometry to accurately determine the distance/voltage relationship. It is also felt that the barrier heights are additionally lowered by water adsorbates on the electrode surfaces. These layers create intermediate tunneling states and an effectively lowered tunnel barrier [13,14]. Further experiments will be conducted to verify this as well.

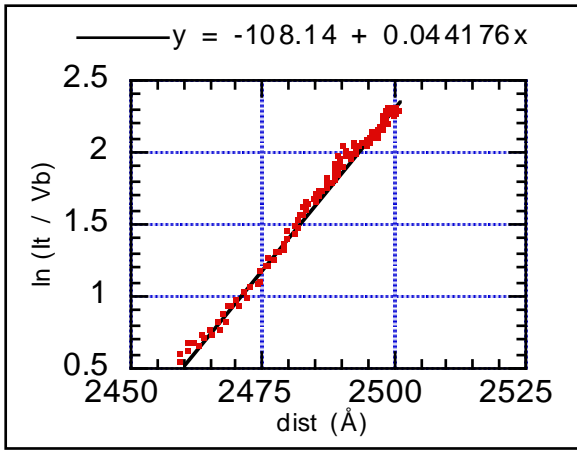


Fig. 7 Log plot of data from Figure 6 showing linear dependence of current on distance.

A careful noise analysis of the system was performed. Following the analysis of Gabrielson [15], the noise sources of the system are considered. This accelerometer is subject to many possible noise sources, but is ultimately limited by thermomechanical noise from the proof mass, as are all accelerometers. This can be easily calculated from Equation 3.

$$a_n = \frac{\omega_o^2}{g} X_n = \frac{\omega_o^2}{g} \sqrt{\frac{4k_b T}{\omega_o^3 m Q}} \quad [3]$$

Given $k_b T = 25$ mV, $m = 5.2$ micrograms for this device, $\omega_o = 2\pi(5.5$ kHz), $g = 9.8$ m/s² and a Q value of 20, which is typical for SCREAM devices in air [16]. g/ω_o^2 is the response factor of the device, 8.1×10^{-9} m/g. Finishing the calculation results in 7.5×10^{-6} g/rt Hz as the acceleration noise of the device.

The device resolution is defined as the minimum signal discernible from the noise floor of the device. The noise can be measured by monitoring the error signal of the feedback circuit with a spectrum analyzer. A typical plot of noise from the DSA is presented in Figure 8. This plot shows $1/f$ noise common to tunneling [5]. Above 5 kHz, noise is seen to be white with a value of 10 μ g/rt Hz. This is near the value predicted by the theoretical calculation of the thermal-mechanical noise of the proof mass.

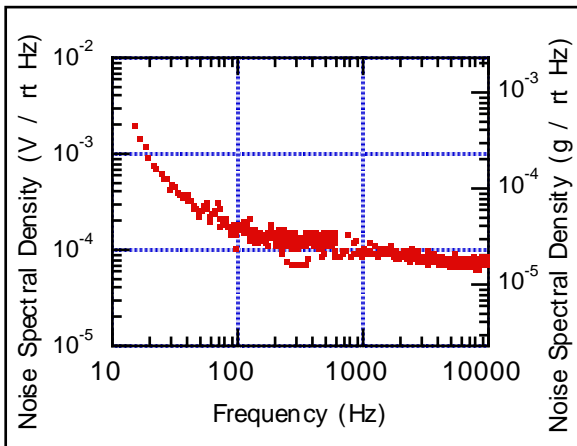


Fig. 8 Plot of noise spectrum. White noise floor level is 10 μ g/rt Hz, set by thermal mechanical noise

Device sensitivity is defined as amount of signal out of a device for a given excitation. For an accelerometer this figure of merit should be expressed in V/g. By differentiating equation [1], we get the displacement to current sensitivity:

$$\frac{dI_t}{dx} = (-\alpha\sqrt{\phi})V_b \exp(-\alpha\sqrt{\phi}) = I_t(-\alpha\sqrt{\phi}) \quad [4]$$

Given that we use a 3.5 nA tunneling current setpoint and typical values of $\phi = 0.2$ eV, $\alpha = 1.025$ 1/(Å \sqrt eV), the displacement to current sensitivity is 5 A/m. The response factor was previously calculated to be 8.1×10^{-9} m/g. With a gain of 2.8×10^7 V/A in the first stage of the feedback circuit, the accelerometer sensitivity is then calculated to be 1.2 V/g. By applying a 10 mg excitation, at 1.5 kHz, with a shake table, the sensitivity is measured to be 0.23 V/g, as seen in Figure 9.

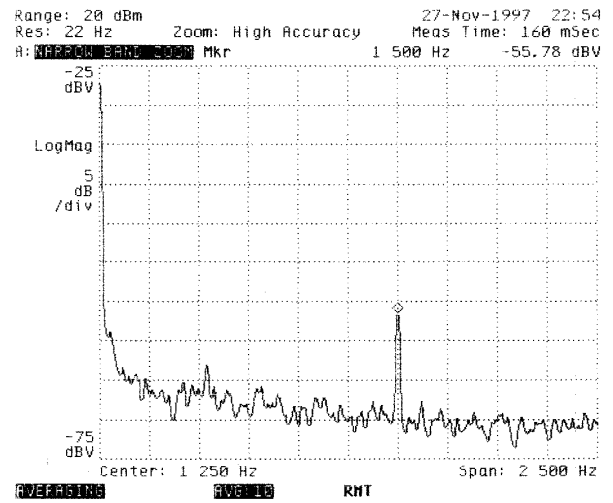


Fig. 9 Frequency spectrum during 1.5 kHz excitation of accelerometer.

CONCLUSION

A lateral tunneling accelerometer has been fabricated in single crystal silicon. Utilizing favorable characteristics of the SCREAM process, a new design with high-aspect-ratio beams and a self-aligned tip has been developed and tested. Tunneling with the sensor has been verified. Signal to noise ratios have been measured consistent with other theory. Excellent performance from this preliminary design points to a bright future for new group of ultra high resolution micromechanical accelerometers utilizing the benefits of the SCREAM process.

ACKNOWLEDGMENTS

The authors wish to thank Professor Thomas Kenny of Stanford for his invaluable advice necessary to accurately represent the results of this research. This research is supported by a grant from DARPA and the NSF. The work was conducted at the Cornell Nanofabrication Facility, Ithaca, NY.

REFERENCES

- [1] K.A. Shaw, Z.L. Zhang, and N.C. MacDonald, "SCREAM-I: A single-mask, single-crystal silicon, reactive ion etching process for microelectromechanical structures," *Sensors and Actuators A*, 40, pp. 63-70 (1994).
- [2] R. P. Van Kampen, Bulk-Micromachined capacitive Servo-Accelerometer, Ch. 1, Delft University Press, Delft, The Netherlands, 1995.
- [3] C.F. Quate, *et al.*, "Tunneling Accelerometer," *Journal of Microscopy*, 152, pp. 73-76 (1988).
- [4] Scheeper, P.R., *et al.*, "Development of a modal analysis accelerometer based on a tunneling displacement transducer," *Transducers '97. International Conference on Solid-State Sensors and Actuators*, Chicago, Ill., v. 2, 3B2.04, pp. 867 (1997).
- [5] T.W. Kenny, W. J. Kaiser, *et al.*, "Micromachined silicon tunnel sensors for motion detection", *Appl. Phys. Lett.*, 58 (1) pp. 100 (1991).
- [6] K. Najafi, *et al.*, "A low-voltage bulk silicon tunneling-based microaccelerometer", *IEEE IEDM 95-593*, 23.1.1 (1995).
- [7] J. Wang, *et al.*, "Design, fabrication, and measurement of a tunneling tip accelerometer," *Solid-State Sensor and Actuator Workshop*, Hilton Head, S.C., USA, pp. 68 (1996).
- [8] R. L. Kubena, *et al.*, "A new miniaturized surface micromachined tunneling accelerometer," *IEEE Electron Device Letters*, 17, No. 6, pp. 306-8 (1996).
- [9] D. Kobayashi, *et al.*, "An integrated lateral tunneling unit," *IEEE MEMS 92*, Travemunde, Germany, pp. 214-19, (February 4-7, 1992).
- [10] W.R. Runyan, K.E. Bean, Semiconductor Integrated Circuit Processing Technology, p. 551, Addison-Wesley Publishing Company, Inc., New York, 1990.
- [11] C.H. Liu, T.W. Kenny, *et al.*, "Characterization of a high-sensitivity micromachined tunneling accelerometer," *Transducers '97. International Conference on Solid-State Sensors and Actuators*, Chicago, Ill, v. 2, pp. 471-2 (1997)
- [12] T.W. Kenny, *et al.*, "Wide bandwidth Electromechanical actuators for tunneling displacement transducers," *J. MEMS*, 3 (3), pp. 97-104, Sept 1994.
- [13] J. Halbritter, "Tunnel channels, spectroscopy, and imaging in STM," *Applied Physics A*, pre-print
- [14] G. Repphun, J. Halbritter, "Tunnel channels, charge transfer and imaging mechanisms in scanning tunneling microscopy," *JVST A* 13(3), p.1693 May/June 1995.
- [15] T. B. Gabrielson, "Mechanical-thermal noise in micromachined acoustic and vibration sensors," *IEEE Trans on Electron Devices*, 40, (5), p.903, May 1993.
- [16] S.A. Miller, K.L. Turner, N.C. MacDonald, "Microelectromechanical scanning probe instruments for array architectures", *Rev. Sci. Instr.*, v. 68 (11) p. 4155, Nov 1997.